Damping Method of High Frequency Resonance for Stator Current Controlled DFIG System under Parallel Compensation Grid

Pang, Bo; Wu, Chao; Nian, Heng; Blaabjerg, Frede

Published in:
I E E E Transactions on Power Electronics

DOI (link to publication from Publisher):
10.1109/TPEL.2020.2975046

Publication date:
2020

Document Version
Accepted author manuscript, peer reviewed version

Damping Method of High Frequency Resonance for Stator Current Controlled DFIG System under Parallel Compensation Grid

Bo Pang, Chao Wu, Heng Nian, *Senior Member, IEEE*, Frede Blaabjerg, *Fellow, IEEE*

***Abstract*—High frequency resonances (HFR) is a subsistent issue in doubly fed induction generator (DFIG) system when it connects to a parallel compensation grid, due to the insufficient phase margin between the impedance of DFIG and grid. The occurrence mechanism and damping methods for the HFR in the rotor current controlled DFIG (RCC-DFIG) have been investigated in the existing literatures, while the appearance and solutions of HFR for the stator current controlled DFIG (SCC-DFIG) have not been studied yet. Based on the impedance of SCC-DFIG, this paper analyzes the occurrence mechanism of the HFR in the SCC-DFIG. Thereby, an impedance reshaping method based on stator voltage feedforward controller (SVFC) is proposed. By employing the proposed SVFC, SCC-DFIG can avoid HFR in a wide frequency range, which signifies that HFR with varied resonance frequency caused by the change of compensation degree can be damped well. More importantly, compared to the exiting solutions for HFR damping, the impedance reshaping effect of the proposed SVFC for SCC-DFIG is irrelevant to the parameters of DFIG, so that the HFR damping controller can be valid for different DFIG systems without redesigning controller parameters. Theoretical analysis and experiments are given to illustrate effectiveness and practicability of the proposed method**

***Index Terms*—damping control, doubly fed induction generator, high frequency resonance, stator current control, stator voltage feedforward.**

I. INTRODUCTION

Wind power generation system based on doubly fed induction generator (DFIG) is being widely applied in renewable power generation, due to the advantages of small converter capacity, independent active and reactive power regulation, as well as variable speed.

However, due to the rapid development of power transmission technical, the distributed grids with comparatively large impedance are replacing the traditional stiff grid to connect to the wind power generation systems [1-4], in which the grid impedance cannot be neglected any more. In addition, as a vital technique to improve the power quality [5-6], reactive compensations have been widely applied in distributed power system. Hence, the operation performance and improved control strategy of the DFIG system which connects to the parallel compensation grid should be considered, though the control techniques of DFIG system under stiff grid [1-2] have been researched a lot.

Several literatures have indicated that when DFIG system connected to a weak grid with a non-ignored impedance, the interactions between DFIG system and grid can result in the instability issues [7-14]. As indicated by impedance stability theory [7-8], resonance occurs when phase angle difference between the impedance of grid connected device and grid close to 180° at the intersection of impedance amplitude. Especially, for parallel compensatory grid, the issue of high frequency resonance (HFR) is a subsistent issue for the grid-connected device [9-11], since impedance of parallel compensation grid has a capacitance characteristic at the high frequency, where the majority of grid connected devices including DFIG behave as an inductive characteristic [10-13]. When HFR occurs, a considerable high frequency component will be introduced into the voltage at point of common coupling (PCC), thus distortions appear in the output current of DFIG so that the power quality cannot satisfy the requirement of grid connections. In addition, the appearance of HFR can severely affect the work conditions of other grid connected devices, which are connected to the same PCC as well. Therefore, for enhancing the stability of interconnected systems, it is essential to guarantee the grid connected DFIG system can have enough phase margin within the high frequency range where HFR may occur.

For damping the HFR exists when DFIG system connects the parallel compensation grid, [10-13] developed the high frequency impedance model based on vector control strategy with rotor current control (RCC) loop, which indicated that the potential frequency of HFR is higher than 500Hz so that the influence of phase locked loop (PLL) can be neglected. As for the HFR damping, [9-12] proposed and active damping control based on resonant regulator, and this method can be effective for DFIG system on the condition that the resonant frequency has been detected accurately, in which the adaptive frequency detection [15]-[16] is achieved by a frequency locked-loop based on the adaptive notch filter (ANF-FLL). However, [14] pointed out that the resonant frequency of HFR will vary when the compensation degree changes, so that the performance of the HFR damping controller in [10-12] will degrade due to the dynamic time delay of the resonance frequency detection [17]-[18]. For overcoming the limitations of the damping methods based on resonant regulator, [13-14] proposed a wideband

This work is supported by the National Natural Science Foundation of China under Grant 51977194.

Bo Pang and H. Nian are with the College of Electrical Engineering, Zhejiang University, Hangzhou, China. (Corresponding author Heng Nian, nianheng@zju.edu.cn).

Chao Wu and Frede Blaabjerg are with the Center of Reliable Power Electronics (CORPE) Department of Energy Technology, Aalborg University, Aalborg, Denmark

control strategy which are effective within the potential HFR frequency range, and resonant frequency detection can be avoided. Therefore, the existing HFR damping method based on VFR can suppress HFR in a wide frequency range, while the existing HFR damping method based on resonator cannot. The core of wideband HFR damping is the bandwidth of the damping controller.

It should be pointed out that the exiting HFR damping methods above are developed for the DFIG system with RCC loop. Compared with the RCC, stator current control (SCC) has also been employed for DFIG control [19-21]. It has been proved [21] that the performance and stability of power control of the two methods are equal. Furthermore, SCC-DFIG has the advantage that parameters of DFIG is not covered in the calculation of the current reference so that the variation of the generator parameters in practice cannot influence the reference calculation in current control [19-20]. However, the issue of HFR in the SCC-DFIG system has not been investigated yet.

The research of HFR damping mainly contain two aspects, the impedance modeling and the impedance reshaping. [14] and this paper both aim at developing the HFR damping control for DFIG system, while the impedance model and the impedance reshaping in the two papers are different, due to different control diagram for DFIG and the different required damping performance.

(1) **The impedance models are different**.

The existing research [14] serves for the closed-loop control for RCC-DFIG, while this paper serves SCC-DFIG. Compared to RCC-DFIG, SCC-DFIG is more robust to the variation of the generator parameters, since the reference calculation in current control is irrelevant to generator parameters [21]. The different control diagrams result in the different impedance model of DFIG system, which is the fundamental difference compared with [14] and new impedance reshaping method should be studied.

(2) **Impedance reshaping methods are different.**

Furthermore, the impedance reshaping method of [14] has a limitation when it is applied in SCC-DFIG. The method of [14] introduces a virtual impedance named VFR in series for DFIG by adding an additional current control loop, the value of VFR equals to the expression of the damping controller. When the VFR in [14] is introduced into the different SCC-DFIG systems without redesigning the controller parameters, the value of the virtual impedance is changeless while the original impedance of DFIG system changes, so that the impedance reshaping effect is affected. For maintaining the impedance reshaping effect, the controller in [14] has to be redesigned, when it is applied for the different DFIG systems.

For solving this issue, this paper develops a different impedance reshaping method based on the stator voltage feedforward control (SVFC), which can introduce an impedance correction factor on the original impedance of DFIG. With the proposed method, no matter how the parameters of DFIG change, the impedance reshaping effect equals to the correction factor, while the correction factor is only related to the proposed damping controller. Therefore, once the controller of the SVFC is designed, it can be effective for the HFR damping in different SCC-DFIG systems without parameter redesign. Table I summarizes the contributions of this paper more intuitively

TABLE I CONTRIBUTION OF THE PROPOSED METHOD

	HFR damping based on VFR [14]	The proposed SVFC
HFR damping	○	○
Adapt to the change of HFR frequency	○	○
Adapt to different DFIG systems	×	○

The structure of this paper can be stated as follow, firstly, in Section II, the impedance of SCC-DFIG will be deduced firstly, then the mechanism of HFR will be analyzed. Section III describes the proposed method based on the impedance of DFIG with SVFC and then a schematic diagram and design procedure of the proposed method will be described. By comparing with the existing damping methods, Section IV evaluates the operation performance of SCC-DFIG after employing the proposed SVFC. The experimental results in Section V verify the effectiveness and the practicability of the proposed damping method. Section VI summarizes the contributions of this paper.

II. HFR ANALYSIS OF STATOR CURRENT CONTROLLED DFIG

A. Impedance modeling of the SCC-DFIG

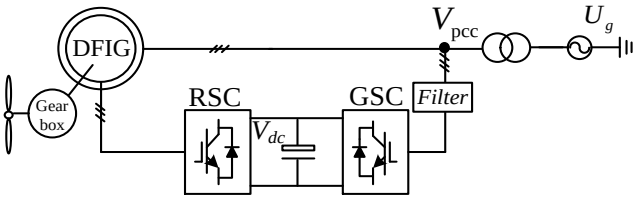

Fig. 1 DFIG system structure

The DFIG system consists of rotor side converter (RSC) and grid side converter (GSC), which are connected via a DC bus as shown in Fig. 1. The DC bus isolates the control of RSC and GSC so that the impedance of DFIG system can be described as the parallel of the two units [4], as shown in Fig. 2. According to [10-14], the HFR damping methods are usually planted at RSC to obtain better damping effect, since stator side impedance dominates impedance of DFIG system. For analyzing the HFR in SCC-DFIG, the impedance model of SCC-DFIG should be deduced firstly, since it is the basis of stability analysis. [4], [9-10] indicate that the influence of PLL for the high frequency impedance of DFIG can be neglected due to its narrow bandwidth, therefore the impedance of SCC-DFIG can be obtained by the control block of DFIG.

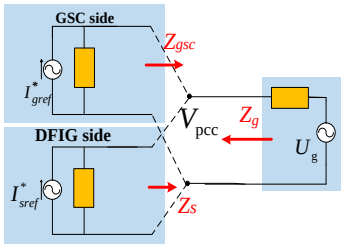

Fig. 2 Equivalent impedance circuit of interconnected system

The equations of stator and rotor voltage of DFIG can be expressed in *dq* frame as [22-23],

$$\begin{cases} \boldsymbol{U}_{sdq} = \dfrac{d\boldsymbol{\psi}_{sdq}}{dt} + j\omega_1\boldsymbol{\psi}_{sdq} + R_s\boldsymbol{I}_{sdq} \\ \boldsymbol{U}_{rdq} = \dfrac{d\boldsymbol{\psi}_{rdq}}{dt} + j\omega_{slip}\boldsymbol{\psi}_{rdq} + R_r\boldsymbol{I}_{rdq} \end{cases} \tag{1}$$

$$\begin{cases} \boldsymbol{\psi}_{sdq} = L_m\boldsymbol{I}_{rdq} + L_s\boldsymbol{I}_{sdq} \\ \boldsymbol{\psi}_{rdq} = L_m\boldsymbol{I}_{sdq} + L_r\boldsymbol{I}_{rdq} \end{cases} \tag{2}$$

where $\boldsymbol{U}_{sdq}$, $\boldsymbol{U}_{rdq}$ and $\boldsymbol{I}_{sdq}$, $\boldsymbol{I}_{rdq}$ are voltages and currents of stator and rotor; ω_1 is synchronous speed, ω_{slip} is rotor speed; R_s, R_r are resistance of stator and rotor, $L_{s\sigma}$ and $L_{r\sigma}$ are leakage inductance of stator and rotor; L_m is magnetic inductance, L_s=L_m+$L_{s\sigma}$, L_s=L_m+$L_{r\sigma}$; $\boldsymbol{\psi}_{sdq}$ and $\boldsymbol{\psi}_{rdq}$ are stator flux and rotor flux.

The stator current in *dq* frame can be obtained as,

$$\boldsymbol{I}_{sdq} = -G_{us}\boldsymbol{U}_{sdq} + G_{ur}\boldsymbol{U}_{rdq} \tag{3}$$

where, L_δ=(L_sL_r-L_m^2)/L_m.

By ignoring the resistance of stator and rotor winding, $G_{us}(s)$ and $G_{ur}(s)$ can be expressed as:

$$\begin{cases} G_{us}(s) = \dfrac{sL_r + j\omega_{slip}}{(s+j\omega_1)(sL_\delta L_m + j\omega_{slip}L_\delta L_m)} \\ G_{ur}(s) = \dfrac{L_m}{sL_\delta L_m + j\omega_{slip}L_\delta L_m} \end{cases} \tag{4}$$

Thus, the mathematical model of SCC-DFIG is expressed as (3)-(4), in which the rotor voltage can be obtained by stator current controller [19-21], which can be described as,

$$\boldsymbol{U}_{rdq} = H_{si}H_d(\boldsymbol{I}^*_{sdq} - \boldsymbol{I}_{sdq}) \tag{5}$$

where, the effect of system delay caused by the sampling and digital control can be expressed by $H_d(s)$= e^{-sT_d}, T_d is 1.5 sampling period, in which one period is the computation delay caused by sampling, another half period represents the delay caused by PWM [24], H_{si} is the current controller.

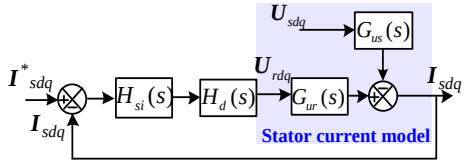

Fig. 3 Block diagram of SCC-DFIG

Thereby, the block diagram of SCC can be illustrated by Fig. 3. The stator current can be expressed as,

$$\boldsymbol{I}_{sdq} = -Y_{sdq}\boldsymbol{U}_{sdq} + H_{sdq}\boldsymbol{I}^*_{sdq} \tag{6}$$

where the physical significance of Y_{sdq} and H_{sdq} are the output admittance of DFIG and the tracking ability of stator current in the *dq* frame.

Combining (3)-(5), the expression of Y_{sdq} can be obtained as,

$$Y_{sdq}(s) = \frac{G_{us}(s)}{1 + G_{ur}(s)H_d(s)H_{si}(s)} \tag{7}$$

Thereby, the impedance Z_s of DFIG system in the stationary reference frame can be expressed as,

$$Z_s(s) = 1/Y_{sdq}(s - j\omega_1) \tag{8}$$

where, the frequency shifting of s-$j\omega_1$ is introduced, which represents the conversion between the rotating *dq* frame and the stationary frame [10-11].

The impedance of the GSC side has been obtained by others [9-14], which can be expressed as (9), L_f and H_{gi}(s) are the filter inductance and current controller of GSC.

$$Z_{gsc} = H_{gi}(s - j\omega_1)H_d(s - j\omega_1) + sL_f \tag{9}$$

The impedance of SCC-DFIG can be obtained as,

$$Z_{DFIG}(s) = Z_s(s)//Z_{gsc}(s) \tag{10}$$

The impedance of the parallel compensation grid [12-14] can be written as follows, in which L_g, R_g and C_g are the grid equivalent inductance, grid equivalent resistance and parallel compensation capacitor, K_e is the ratio of transformer.

$$Z_g = K_e^2\frac{sL_g + R_g}{s^2L_gC_g + sC_gR_g + 1} \tag{11}$$

B. HFR analysis for SCC-DFIG system

Based on the impedance expressions of the SCC-DFIG system and the parallel compensation grid, the mechanism of HFR in SCC-DFIG system and problems of the existing HFR damping method will be analyzed in this section.

TABLE II PARAMETERS OF DIFFERENT INTERCONNECTED SYSTEMS

2 MW DFIG system

DFIG system				
S_n/MVA	U_n/kV	R_r(pu)	$L_{s\sigma}$(pu)	L_m(pu)
2	0.69	0.00121	0.11	11.3
R_s(pu)	$L_{r\sigma}$(pu)	L_f/mH		
0.0108	0.102	0.9		
Parallel compensation grid				
R_g/ohm	U_g/kV	f_g/Hz	C_g/μF	L_g/H
0.05	10	50	1	0.036

1 kW DFIG system

DFIG system				
S_n/kVA	U_n/kV	R_r/Ω	$L_{s\sigma}$/mH	L_m/mH
1	0.11	0.88	2.2	87.5
R_s/Ω	$L_{r\sigma}$/mH	L_f/mH		
1.01	2.4	8		
Parallel compensation grid				
R_g/Ω	U_g/kV	f_g/Hz	C_g/μF	L_g/mH
0.005	0.11	50	18	2

Impedance curves for different DFIG systems are illustrated in Fig. 4, in which the parameters of DFIG systems and parallel compensation grids can be seen in Table II, which represents to illustrate the problem in different power levels. Fig. 4 (a) illustrates the impedance curve of 2 MW DFIG system, there are two amplitude intersections P_1 and P_2, phase difference between the impedance of DFIG system and parallel compensation grid is 179° at P_2 (875Hz), which indicates that a 875 Hz HFR exists in the interconnected system, while for the 1 kW DFIG system in Fig.4 (b), one of the amplitude intersections P_4 (880Hz) is an unstable point as well, since the phase difference between the impedance of DFIG system and parallel compensation grid is 176° at P_4, which indicates that a 880 Hz HFR exists in the interconnected system. It can be found that SCC-DFIG system still has the issue of HFR when it is connected to parallel compensated grid. Here should be noted

that, according to the research of [13], the 2MW case is very close to a diverging resonance, which can be called the critical stable point. While for the latter case, there is still an equivalent resistance characteristic exists in the DFIG system. Therefore, although the phase margins of the two interconnected are both insufficient, the equivalent resistance of the 1kW DFIG system can cause the different harmonic components of HFR.

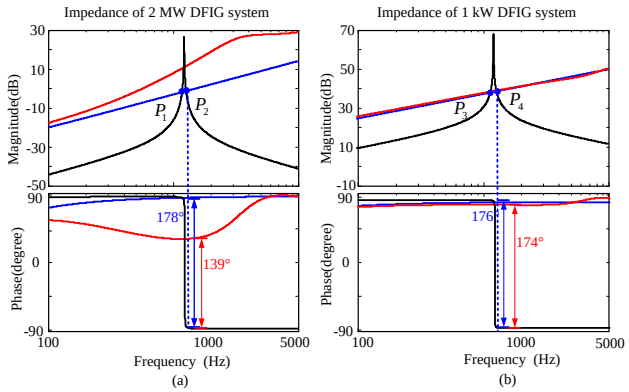

Fig. 4 Impedance curves of different DFIG systems

Impedance of parallel compensation grid Z_g

Impedance of DFIG system Z_{DFIG}

Reshaped impedance of the DFIG system Z_{DFIG_re}

As stated in the Introduction, the existing HFR damping methods are equivalent to introduce a fixed value virtual impedance Z_v [12-14], as shown in Fig. 5.

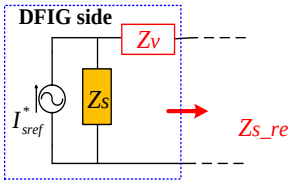

Fig. 5 Impedance reshaping of the existing method

Define λ as the coefficient of impedance reshaping for DFIG. It can be indicated that the virtual impedance with the beforehand designed value can effectively reshape the impedance of DFIG system in order to obtain a specific λ. However, for obtaining a specific λ, which can effectively reshape the DFIG impedance to guarantee a sufficient phase margin for the interconnected system, the required Z_v can be expressed as,

$$\lambda = \frac{Z_{s\_re}}{Z_s} = \frac{Z_s + Z_v}{Z_s} = 1 + \frac{Z_v}{Z_s} \tag{12}$$

$$Z_v = Z_s(\lambda - 1) \tag{13}$$

which signifies virtual impedance should be designed according to Z_s when λ is known, while Z_s depends on the parameters of DFIG, so that the introduced Z_v in different DFIG systems should be different according to the parameters of the DFIG.

Here take the HFR damping controller in [14] as an example, of which the expression can be written as,

$$H_{damp} = H_{filter}(-s^2) \tag{14}$$

where H_{filter} is a five orders Chebyshev filter, where the cut-off frequency f_{cut} = 50Hz and coefficient of fluctuation is 0.5.

When the damping controller is planted in the 2MW DFIG system, impedance curve of DFIG system can be reshaped effectively, as shown in Fig. 4 (a), in which the phase difference at HFR point can be reshaped to 139°. The HFR at 875Hz can be damped effectively. However, when the damping controller is applied to the 1 kW DFIG system directly without parameters redesign, the phase difference at P_4 only can be decreased to 174°, so that the HFR cannot be damped well.

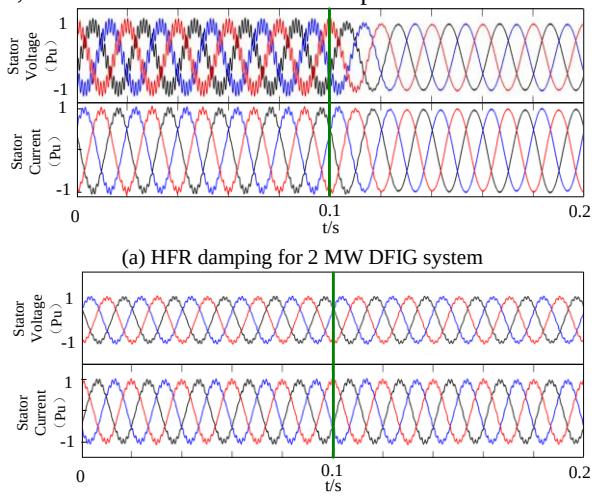

Fig. 6 HFR damping effect of the existing method for different DFIG systems

Fig. 6 illustrates the operation results of the different DFIG systems to validate the analysis above. In Fig. 6(a), when the 2 MW DFIG system connects to a parallel compensation grid, an 875 Hz resonance occurs, in which the components of HFR in stator voltage U_s and stator current I_s are 28.3% and 7.0% respectively. After planting the HFR damping controller [14], the components of the HFR in U_s and I_s are suppressed to 1.1% and 0.8% respectively, which means HFR can be damped effectively. When the damping controller without parameters redesign is applied in the 1kW DFIG system, as shown in Fig. 6 (b), the components at 880 Hz HFR in U_s and I_s only can be suppressed to 6.3% and 6.6% from 7.7% and 7.7%, which means that the HFR damping controller is not working properly in this occasion.

Thus, it can be summarized that,

(1) When the DFIG is connected to a parallel compensation grid, HFR is a potential issue for the SCC-DFIG system as well as RCC-DFIG system, so an HFR damping method should be developed for SCC-DFIG to guarantee stability of the interconnected system.

(2) The existing damping methods introduce a virtual impedance with fixed value to effectively reshape the impedance of DFIG. When the controlled object varies, the damping controller has to be redesigned, otherwise HFR damping may not be working.

Therefore, this paper proposes an HFR damping method based on stator voltage feedforward controller (SVFC) for the SCC-DFIG, which will be described detailly in next section. The proposed SVFC can introduce a correction factor instead of a fixed value virtual impedance on the original impedance of DFIG system, so that the impedance reshaping effect is irrelevant to the controlled object. Therefore, the parameter dependence on DFIG can be avoided for the HFR damping.

III. PROPOSED HFR DAMPING METHOD BASED ON SVFC

To present effectiveness and advantage of the proposed method, this section analyzes the operation mechanism of the proposed HFR damping method based on SVFC firstly, then the implementation and design procedure of SVFC will be described. Fig. 7 illustrates the control block of DFIG system after introducing SVFC, in which the rotor voltage of DFIG can be rewritten as,

$$\boldsymbol{U}_{rdq} = H_{si}H_d(\boldsymbol{I}^*_{sdq} - \boldsymbol{I}_{sdq}) + G_{SVF}\boldsymbol{U}_{sdq} \quad (15)$$

where G_{SVF} is the equivalent transfer function of stator voltage feedforward path.

Thereby the stator current can be rewritten as,

$$\boldsymbol{I}_{sdq\_SVF} = -Y_{sdq\_SVF}\boldsymbol{U}_{sdq} + H_{sdq\_SVF}\boldsymbol{I}^*_{sdq} \quad (16)$$

where Y_{sdq_SVF} and H_{sdq_SVF} represent the output admittance of DFIG and the tracking ability of stator current in dq frame after introducing the stator voltage feedforward.

$$Y_{sdq\_SVF}(s) = (1 - G_{SVF}(s)\frac{G_{ur}(s)}{G_{us}(s)})\frac{G_{us}(s)}{1 + G_{ur}(s)H_d(s)H_{si}(s)} \quad (17)$$

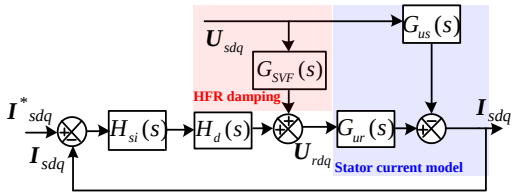

Fig. 7 Block diagram of stator current control without SVFC

G_{ur}/G_{us} in high frequency can be expressed as,

$$\frac{G_{ur}(s)}{G_{us}(s)} = \frac{L_m}{L_r}\frac{s + j\omega_1}{s + j\omega_{slip}/L_r} \approx 1 \quad (18)$$

Thus, the reshaped impedance in the stator side of DFIG can be rewritten as,

$$Z_{s\_SVF}(s) = \frac{1}{Y_{sdq\_SVF}(s - j\omega_1)} = \frac{1}{1 - G_{SVF}(s - j\omega_1)}Z_s(s) \quad (19)$$

It can be seen by (16) that, when the SVFC is introduced, the impedance reshaping coefficient λ can be expressed as,

$$\lambda = \frac{1}{1 - G_{SVF}(s - j\omega_1)} \quad (20)$$

It can be also found that the stator voltage feedforward has the capability to reshape impedance of DFIG, more importantly, λ is irreverent to the parameters of the DFIG, and which verifies that the effect of impedance reshaping can be maintained even if the control object varies.

It should be noted that, according to (21)-(22), Z_{s_SVF} can be divided into two parts, i.e., Z_s and Z_v'. Thus, the proposed SVFC can be described in the form of series virtual impedance as well, as shown in Fig .8 (b).

$$Z_{s\_SVF}(s) = Z_s(s) + \frac{G_{SVF}(s - j\omega_1)}{1 - G_{SVF}(s - j\omega_1)}Z_s(s) = Z_s(s) + Z_v'(s) \quad (21)$$

$$Z_v'(s) = \frac{G_{SVF}(s - j\omega_1)}{1 - G_{SVF}(s - j\omega_1)}Z_s(s) \quad (22)$$

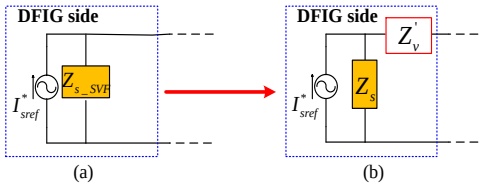

Fig. 8 Impedance reshaping of the proposed method

Compared to the existing method which introduces a fixed virtual impedance, the proposed method is equivalent to introduce a variable virtual impedance Z_v', and the value of Z_v' is variable in different DFIG systems, even if the damping controller G_{SVF} is fixed. Thus, if the controlled DFIG changes, the proposed damping method always can be equivalent to introduce a virtual impedance which is matched for Z_s.

The implementation of the proposed HFR damping method based on SVFC is illustrated in Fig. 8. On the basis of the fundamental control loop, an additional stator voltage feedforward path is introduced. The detailed descriptions for the two control loops can be presented as follows.

1). Fundamental control loop

The control system is developed in the synchronous dq frame, so frequency and electrical angle of fundamental grid voltage are obtained by PLL on synchronous dq frame. The RSC is responsible for the maximum power point tracking, while GSC is responsible for guaranteeing the constant DC voltage, the stator current reference can be calculated by the power reference. Considering that the fundamental component of u_{sq} is zero when the grid voltage orientation is employed, the calculation of the current reference can be described as (23), while the current reference of the GSC side is generated by the DC voltage outer loop.

$$\begin{cases} i^*_{sd} = P^*_s / u_{sd} \\ i^*_{sq} = Q^*_s / u_{sd} \end{cases} \quad (23)$$

2). HFR damping control

As illustrated in Fig.9, the stator voltage feedforward in Fig. 7 can be achieved by introducing a SVFC G_{SVFC}(s), in which the relationship between G_{SVFC}(s) and G_{SVF}(s) can be described as,

$$G_{SVF}(s) = G_{SVFC}(s)H_d(s) \quad (24)$$

Phase amendment is one of the cores for the design for damping controller, while also the effective frequency range is another core of the damping controller design. Thus, in order to design G_{SVFC}(s), two aspects including effective frequency range and phase regulation should be considered. Firstly, the effective frequency range of G_{SVFC}(s) should be restricted for isolating high frequency noise, the control effect of the HFR damping controller should be cut-off when the frequency beyond the frequency range of impedance reshaping. Therefore, a low-pass filter G_f(s) should be covered. Considering that the switching frequency of DFIG system can be from 2 kHz to 3 kHz, therefore a second order lowpass filter of which cut-off frequency with 2 kHz is employed, which can be described as,

$$G_f(s) = \frac{\omega_n^2}{s^2 + 1.4\omega_n s + (\omega_n)^2} \quad (25)$$

where ω_n=4000 π/rad

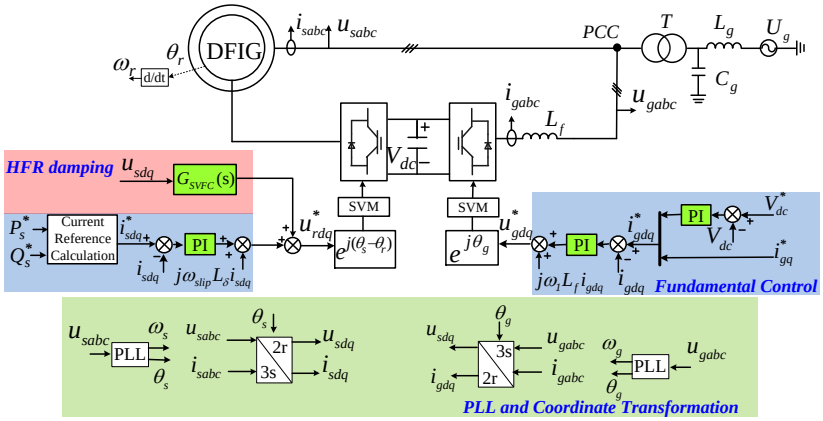

Fig. 9 Control block of the proposed HFR damping method based on stator voltage feedforward

Meanwhile, a phase amendment component should be covered to regulate the phase of DFIG impedance, therefore a lead-lag component $G_R(s)$ is employed, which is the commonly used in a phase regulation component and it can be expressed as,

$$G_R(s) = \left(\frac{s+\omega_a}{s+\omega_b}\right)^n \tag{26}$$

where ω_a and ω_b correspond to the effective frequency range of phase amendment, thus ω_a and ω_b are selected as 1000 π/rad and 4000 π/rad respectively, since the existing literatures [9-14] have indicated that frequency of HFR is higher than 500 Hz. n is the order of $G_R(s)$.

Thus, the maximum phase amendment of $G_R(s)$ φ_{max} can be represented as,

$$\varphi_{\max}(G_R) = n\arctan\left(\frac{\omega_b-\omega_a}{2\sqrt{\omega_a\omega_b}}\right) \tag{27}$$

When the higher order is selected, the larger phase amendment can be provided by $G_R(s)$, while the implementation of digital control is more complicated. Therefore, this paper selects n=2, thus φ_{max}=73°.

The damping controller based on SVFC can be expressed as,

$$G_{SVFC}(s) = G_f(s)G_R(s) \tag{28}$$

IV. Performance Analysis of the Proposed SVFC

This section will analyze the operation performance of the proposed SVFC. Impedance reshaping for different DFIGs is firstly given to illustrate effectiveness and advantage of the proposed control strategy. Then, comparisons between the proposed SVFC and the existing damping method are illustrated to demonstrate the strength of the theoretical analysis.

A. Impedance reshaping effect of the proposed SVFC

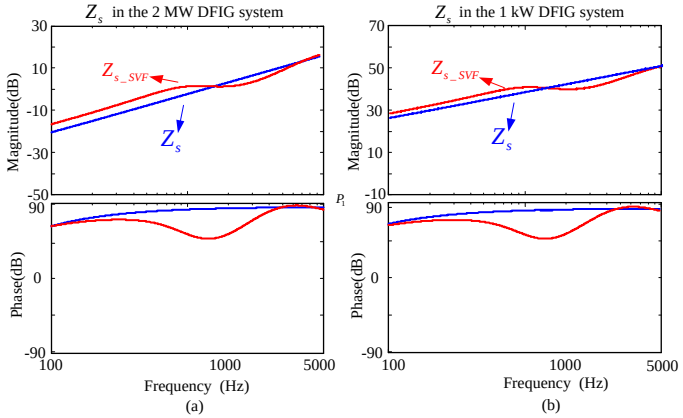

Fig. 10 Impedance curves of Z_s in different DFIGs

Fig. 10 illustrates the effect of the impedance reshaping for DFIG, in which Z_s represents the original impedance of stator side in DFIG system, Z_{s_SVF} represents the reshaped impedance of stator side in DFIG system after planting the proposed SVFC. As shown in Fig. 10, though the SVFC is located in different DFIGs, the effect of impedance reshaping is same, which is corresponds to the conclusion of (19)-(20) where the effect of the impedance reshaping is irrelevant to the DFIG parameters.

Fig. 11 (a) illustrates the reshaped impedance of 2 MW DFIG system Z_{DFIG_SVF} with the proposed SVFC, phase of Z_{DFIG_SVF} can be reshaped effectively, the phase difference between impedance of DFIG system and parallel compensation grid at P_2 can be adjusted to 142°, which means the phase margin at P_2 is 38°, so that the HFR can be avoided. While for the 1 kW DFIG system in Fig. 11 (b), after applying the proposed SVFC, phase difference between the impedance of DFIG system and parallel compensation grid at P_4 can be regulated to be 145°, which signifies the phase margin of 35° can be obtained to guarantee stability of the 1 kW interconnected system.

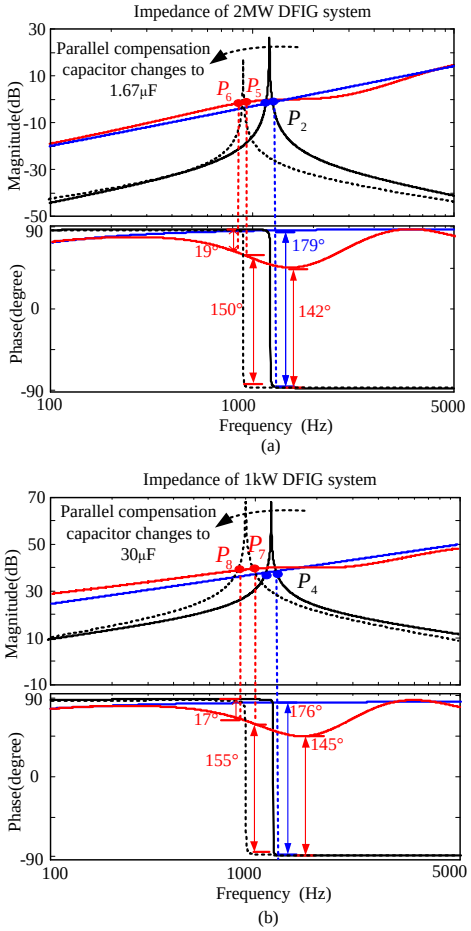

Fig. 11 Reshaped impedance curves of different DFIG systems

- Impedance of grid Z_g
- Impedance of grid Z_g (C_g varies)
- Impedance of DFIG system Z_{DFIG}
- Reshaped impedance of the DFIG system Z_{DFIG_SVF}

In order to reveal the performance of the proposed damping method under different grid compensation degree, Fig. 11 illustrates the impedance of parallel compensation grid when the parallel compensation capacitor varies. As shown in Fig. 11 (a), when the parallel compensation degree changes to 15% from 20%, the amplitude intersections shift to P_5 and P_6, where the phase difference between the impedance of 2MW DFIG system and the grid are 150° and 19° respectively, which reveals that a phase margin of 30° which can be guaranteed for the interconnected system. As to the 1 kW interconnected system, when the parallel compensation capacitor changes to 15%, the amplitude intersection points are P_7 and P_8 where the phase difference are 155° and 17°, in which a phase margin of 25° can be guaranteed for the 1 kW interconnected system.

Thus, it can be concluded that the proposed SVFC has the adaptability for different grid conditions, more importantly, the effect of impedance reshaping can be maintained when the controlled object varies, so that the designed SVFC is effectively for different DFIG systems without parameters redesigning.

B. Comparison between the proposed SVFC and the existing HFR damping controller

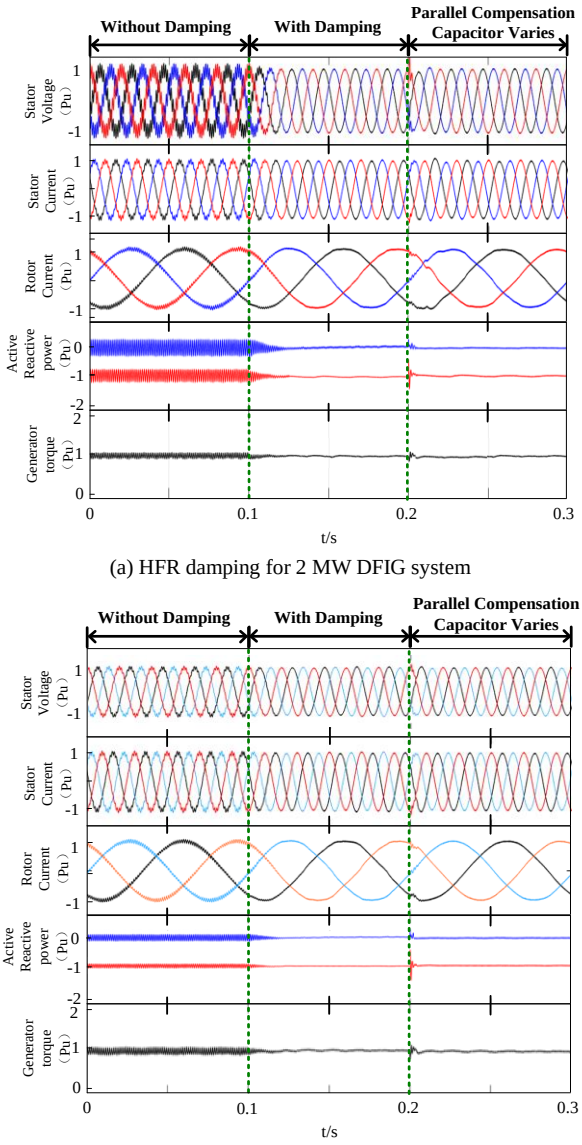

(a) HFR damping for 2 MW DFIG system

(b) HFR damping for 1 kW DFIG system

Fig. 12 The proposed HFR damping effect of different DFIG systems

Fig. 12 illustrates performance of the proposed SVFC for different DFIG systems. Fig. 12(a) and (b) are corresponding to the conditions of 2MW DFIG system and 1 kW DFIG system in Fig. 6 (a) and (b). For the 2 MW interconnected system, when the proposed HFR damping method is enabled at 0.1s, the 875 Hz HFR can be damped within 10ms, the components of HFR in U_s and I_s can be suppressed to 1.0% and 0.6% from 28.0% and 7.0% respectively, and the ripples in active power, reactive power and generator torque can be suppressed to 0.8%, 0.6%, 1.0% from 12.2%, 16.0%, 78.0% respectively, when the parallel compensation capacitor varies to 1.67μF at 0.2s, the interconnected system is stable within 4ms, which demonstrates the analysis of Fig. 10.

For the 1kW DFIG system, the proposed damping controller still can be effective, which is superior to the operation performance of Fig. 6 (b). In Fig. 12 (b), the components of HFR in U_s and I_s can be suppressed to 1.0% and 0.7% from 7.7% and 7.7% respectively when the proposed SVFC is enabled at 0.1s, thereby ripples in active power and reactive power can be

suppressed from 5.0%, 6.0% to 1.0% and 0.9%, meanwhile the generator torque can be damped to 1.0%.

Table III Comparisons of the existing damping method and the proposed SVFC method

		THD of U_s	*THD of I_s*	HFR damped
The existing method	2 MW	1.2%	0.9%	○
	1 kW	6.3%	6.6%	×
The proposed SVFC	2 MW	1.1%	0.7%	○
	1 kW	1.0%	0.80%	○

Table III presents comparison of the existing damping method [14] and the proposed SVFC method, in which the THD in U_s and I_s of DFIG with the damping method are given. It can be indicated by Fig. 12 and Table II that the proposed SVFC can be effective for different DFIG systems, while the existing method cannot be effective without redesigning parameters of damping controller.

C. Analysis for the co-existence of the proposed SVFC and the harmonics suppression for DFIG

Generally, the harmonic voltage exists in grid as well as parallel compensation [14], thus the HFR damping controller should be well co-existed with the controller of harmonics suppression. In view of the resonant controller is the most commonly used method of harmonics suppression [9-13], the fact that the proposed HFR damping method can co-exist with the harmonic suppression controller is proved in this paper.

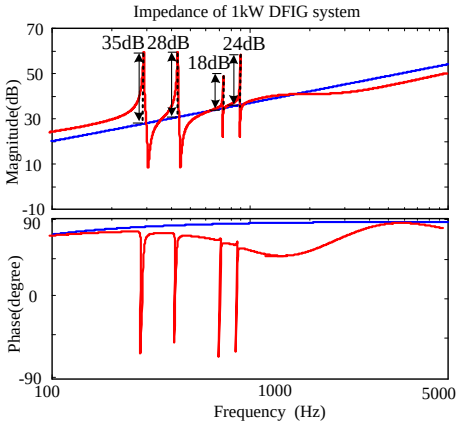

Fig. 13 Impedance curve of DFIG with the proposed SVFC and harmonics suppressor

Fig. 13 illustrates the impedance curve of a 1kW DFIG system with the proposed damping controller and the existing harmonics suppression controller, in which the harmonics suppression controller is planted in an additional current loop in the current control of DFIG [25]. In terms of impedance phase, the phase amendment for DFIG can be maintained, compared to the Fig. 10 of the original paper, which means the HFR damping can be achieved in this situation. In terms of impedance magnitude, the magnitude of the reshaped DFIG impedance increase 35dB, 28dB, 18dB and 24dB at the frequency of -5th ,+7th ,-11th ,+13th , which means the harmonics suppression capability can be improved for the DFIG system. Thus, it can be concluded that the proposed damping controller can well co-exist with the existing harmonics suppression, which also means that the proposed method is suitable for the DFIG connected to parallel compensation grid with harmonics.

V. Experimental Verification

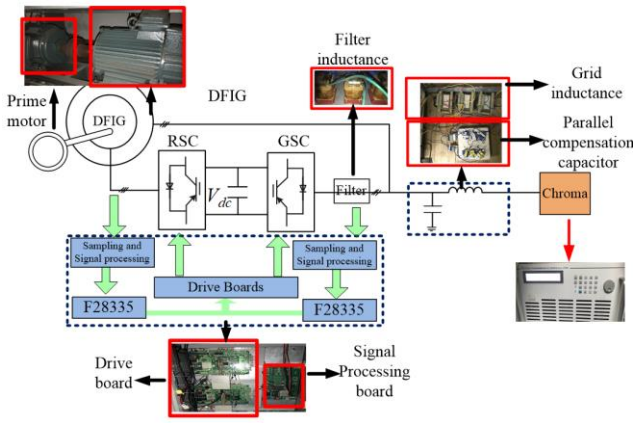

Fig. 14 Schematic diagram of the experimental setup

For verifying the effectiveness of the proposed HFR damping control strategy based on SVFC, the experimental results are given based on a 1 kW DFIG system, of which the parameters are given in Table RIII. The rotor is driven by a prime motor, while the prime motor is controlled by the SB70G7.5 variable-frequency drive. The AC grid source is implemented by a three-phase programmed source Chroma 61704, parameters of grid inductance and parallel compensation capacitor can be seen in Table II. RSC and GSC are controlled by TI TMS320F28335 DSPs to process the electric signals and generate the drive signals.

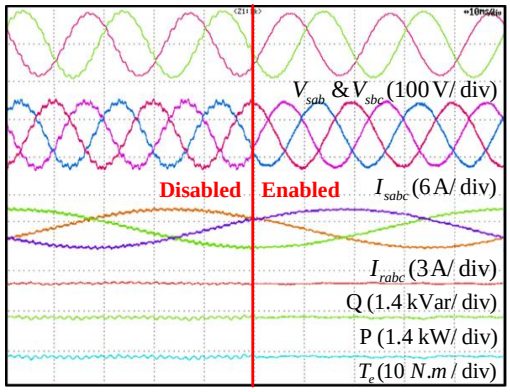

Fig. 15 Operation of DFIG system connects to parallel compensation grid

Fig. 15 shows the operation of DFIG system connected to the parallel compensation grid, in which the rotor speed is 0.8pu, the active power is 1 kW. Corresponding to the analysis of Fig. 4, the DFIG system suffers the 880 Hz HFR so that the voltage at PCC V_s and the output current of DFIG I_s are deteriorated seriously, in which the THD of V_s and I_s are 6.8% and 8.2% respectively, while ripples of 5.0%, 6.0% and 5.7% exist in the active power, reactive power and generator torque.

After employing the proposed HFR damping method based on SVFC, the operation of DFIG system can be improved significantly as illustrated in Fig. 15 as well. The 880Hz HFR can be damped effectively, in which the THD of V_s and I_s can be decreased to 0.6% and 1.3% respectively, meanwhile the ripples in active power, reactive power and generator torque can be reduced to 1.2%, 1.3% and 1.9% respectively. It can be seen in Fig. 15 that the proposed method based on SVFC has good steady state performance for HFR damping.

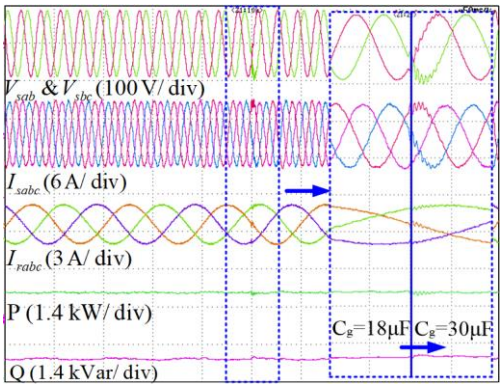

Fig. 16 Performance of the proposed SVFC when the grid condition varies

Furthermore, in order to investigate the performance of the proposed method based on SVFC when the grid condition varies, Fig. 16 illustrates operation of DFIG system with the proposed SVFC when the grid compensation capacitor changes to 30 μF. The THD of V_s and I_s are 0.6% and 1.2% when the parallel compensation degree from 20% to 15%, which signifies the stability of DFIG system can be maintained. Also, the partial enlargement waveform is illustrated as well, the transient process due to the capacitor switching can be limited within 5 ms, which indicates that the proposed HFR damping method has a good transient performance for the variation of the grid conditions.

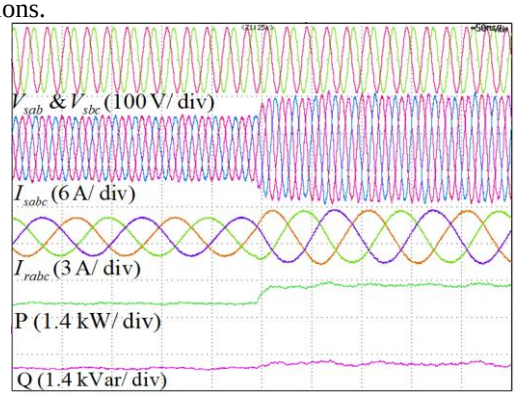

Fig. 17 Power regulation of DFIG system with the proposed SVFC

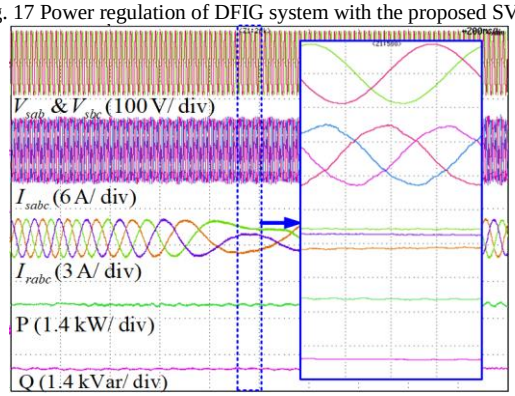

Fig. 18 Speed regulation of DFIG system with the proposed SVFC

Moreover, the power regulation and speed regulation of DFIG system with the proposed HFR damping controller are illustrated in Fig. 17 and Fig. 18 respectively. Active power reference is regulated from 1.0kW to 1.6kW in Fig. 17, where the regulation of power generation can be accurate on the basis of the proposed HFR damping method, which signifies the fundamental control performance will not be affected. While for the speed regulation in Fig. 18, DFIG system can be stable when rotor speed accelerates from 0.8 pu to 1.2 pu, also the partial enlargement waveform at synchronous speed is illustrated to validate the stability of DFIG system when regulating rotor speed.

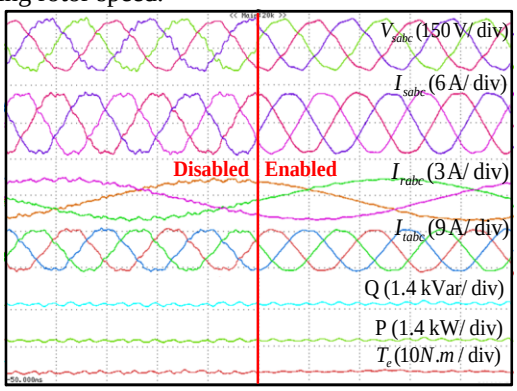

Fig. 19 Performance verification of HFR damping

Fig. 19 illustrates the operation of the DFIG system with proposed damping control and harmonics suppression control, in which harmonic suppression is achieved by the resonant controllers [25-26]. In Fig. 19, grid condition is corresponding to the Fig. 13, grid contains a 30μF parallel compensation capacitor and voltage harmonics. Before enabling the proposed method, grid voltage contains HFR component and harmonics components, the content of HFR at 645Hz is 4.40%, the contents of -5th +7th, -11th and +13th orders harmonics are 2.3%, 1.8%, 1.3% and 1.1% respectively. On this occasion, the THD of I_{sabc} is 7.1%, in which the component of HFR is 3.8%. After enabling the proposed HFR damping method and the harmonics suppression, the HFR components in V_{sabc} and I_{sabc} can be eliminated effectively by the proposed damping control. Meanwhile the THD of I_{sabc} can be reduced to 1.9%, since the harmonics in I_{sabc} are effectively suppressed by the harmonic suppression controller. It can be concluded that the proposed damping method can be suitable for the DFIG system connected to parallel compensation grid with harmonics, and the harmonic suppression can also be achieved.

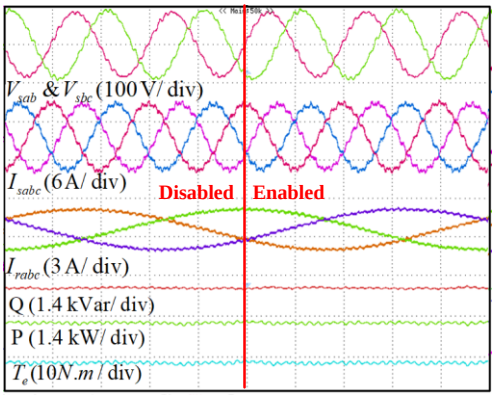

Fig. 20 The existing HFR damping control [13] for 1kW system

Fig. R20 shows the performance of the existing HFR damping method in [14]. For the existing damping controller of [14], when it is designed for 2MW DFIG, it is invalid for a 1kW DFIG, the 880Hz HFR cannot be damped effectively. It is corresponding to the analysis of Fig.4 and the simulation results in Fig. 6.

VI. CONCLUSION

This paper investigates HFR mechanism of SCC-DFIG system, and proposes an HFR damping method based on SVFC, the contributions of this paper can be summarized as follows,

1) Impedance modeling for SCC-DFIG and HFR mechanism in SCC-DFIG system. Firstly, this paper derives the analytical impedance model of SCC-DFIG system, and investigates the HFR mechanism in the SCC-DFIG system. The analytical impedance model and the HFR mechanism of the SCC-DFIG provides the theoretical basis of the proposed impedance reshaping method of SCC-DFIG.

2) Problem of the exiting damping methods. Thereby, this paper investigates the effectiveness of the existing HFR damping methods when they are employed for SCC-DFIG. It was indicated that, the existing HFR damping methods can introduce a virtual impedance in series with the original impedance of DFIG, which will cause that the introduced virtual impedance and the original impedance simultaneously affect the impedance reshaping. Thus, for maintaining the effectiveness of impedance reshaping, the introduced virtual impedance should be different in the different DFIG system. In summary, only if the control parameters in damping controller is redesigned to adapt the different DFIG systems, the existing HFR damping methods can be effective for different DFIGs.

3) An HFR damping method based on SVFC. This paper develops an HFR damping method based on SVFC for SCC-DFIG, it can introduce an impedance correction factor on the original impedance by employing the SVFC, so that the proposed SVFC can be effective for different DFIG systems without parameters re-tuning. Also, the design procedure of the damping controller is fully analyzed and verified.

REFERENCES

[1] M. Liserre, R. Cárdenas, M. Molinas, and J. Rodriguez, "Overview of multi-MW wind turbines and wind parks," *IEEE Trans. Ind. Electron*., vol. 58, no. 4, pp. 1081–1095, Apr. 2011.

[2] R. Cardenas, R. Pena, S. Alepuz and G. Asher, "Overview of Control Systems for the Operation of DFIGs in Wind Energy Applications," *IEEE Trans. Ind Electron*, vol. 60, no. 7, pp. 2776-2798, Jul. 2013.

[3] A. Adib, B. Mirafzal, X. Wang and F. Blaabjerg, "On Stability of Voltage Source Inverters in Weak Grids," *IEEE Access*, vol. 6, pp. 4427-4439, 2018.

[4] Y. Song and F. Blaabjerg, "Overview of DFIG-Based Wind Power System Resonances Under Weak Networks," *IEEE Trans. Power Electron*., vol. 32, no. 6, pp. 4370-4394, June 2017.

[5] A. Shukla, A. Ghosh and A. Joshi, "Hysteresis Current Control Operation of Flying Capacitor Multilevel Inverter and Its Application in Shunt Compensation of Distribution Systems," *IEEE Trans. Power Delivery.*, vol. 22, no. 1, pp. 396-405, Jan. 2007.

[6] R. G. Wandhare and V. Agarwal, "Reactive Power Capacity Enhancement of a PV-Grid System to Increase PV Penetration Level in Smart Grid Scenario," *IEEE Trans. Smart Grid.*, vol. 5, no. 4, pp. 1845-1854, July 2014.

[7] M. Cespedes and J. Sun, "Impedance Modeling and Analysis of Grid Connected Voltage-Source Converters," *IEEE Trans. Power Electron*., vol. 29, no. 3, pp. 1254-1261, Mar. 2014

[8] J. Sun, "Impedance-based stability criterion for grid-connected inverters", *IEEE Trans. Power Electron*., vol. 26, no. 11, pp. 3075-3078, Nov. 2011

[9] Y. Song, X. Wang and F. Blaabjerg, "High-Frequency Resonance Damping of DFIG-Based Wind Power System Under Weak Network," *IEEE Trans. Power Electron.*, vol. 32, no. 3, pp. 1927-1940, March 2017.

[10] Y. Song, F. Blaabjerg and X. Wang, "Analysis and comparison of high frequency resonance in small and large scale DFIG system," *2016 IEEE Energy Conversion Congress and Exposition (ECCE)*, Milwaukee, WI, 2016, pp. 1-8.

[11] Y. Song, F. Blaabjerg and X. Wang, "Analysis and Active Damping of Multiple High Frequency Resonances in DFIG System," *IEEE Trans.Energy Convers.*, vol. 32, no. 1, pp. 369-381, March 2017.

[12] Y. Song, X. Wang and F. Blaabjerg, "Doubly Fed Induction Generator System Resonance Active Damping Through Stator Virtual Impedance," *IEEE Trans. Ind. Electron*, vol. 64, no. 1, pp. 125-137, Jan. 2017.

[13] Y. Song and F. Blaabjerg, "Analysis of the Behavior of Undamped and Unstable High-Frequency Resonance in a DFIG System," *IEEE Trans. Power Electron*., vol. 32, no. 12, pp. 9105-9116, Dec. 2017

[14] H. Nian and B. Pang, "Stability and Power Quality Enhancement Strategy for DFIG System Connected to Harmonic Grid with Parallel Compensation," *IEEE Trans. Energy Convers.*, vol. 34, no. 2, pp. 1010-1022, June 2019.

[15] J.-S. Park, T. H. Nguyen, and D.-C. Lee, "Advanced SOGI-FLL scheme based on fuzzy logic for single-phase grid-connected converters," *J. Power Electron.*, vol. 14, no. 3, pp. 598–607, May. 2014.

[16] H. A. Mohammadpour and E. Santi, "Optimal adaptive sub-synchronous resonance damping controller for a series-compensated doubly-fed induction generator-based wind farm," *IET Renewable Power Generation*, vol. 9, no. 6, pp. 669-681, Aug. 2015.

[17] M. Ciobotaru, R. Teodorescuand, F. Blaabjerg. A new single-phase PLL structure based on second order generalized integrator[C]//*IEEE Power Electronics Specialists Conference.* Jeju, 2006, pp. 1-6.

[18] X. Guo, W. Wu, Z. Chen. Multiple complex coefficient-filter-based phase-locked loop and synchronization technique for three-phase grid-interfaced converters in distributed utility networks[J] .*IEEE Trans. Ind. Electron*., vol.58, no.4: pp.1194-1204, Apr2011.

[19] P. Cheng, H. Nian, C. Wu and Z. Q. Zhu, "Direct Stator Current Vector Control Strategy of DFIG Without Phase-Locked Loop During Network Unbalance," *IEEE Trans. on Power Electron*, vol. 32, no. 1, pp. 284-297, Jan. 2017.

[20] C. Wu and H. Nian, "Stator Harmonic Currents Suppression for DFIG Based on Feed-Forward Regulator Under Distorted Grid Voltage," IEEE Trans. on Power Electron, vol. 33, no. 2, pp. 1211-1224, Feb. 2018.

[21] A. Dòria-Cerezo, M. Bodson, C. Batlle and R. Ortega, "Study of the Stability of a Direct Stator Current Controller for a Doubly Fed Induction Machine Using the Complex Hurwitz Test," *IEEE Trans. Control Sys Tech*, vol. 21, no. 6, pp. 2323-2331, Nov. 2013.

[22] J. Hu, Y. He, L. Xu and B. W. Williams, "Improved Control of DFIG Systems During Network Unbalance Using PI–R Current Regulators," *IEEE Trans. Ind. Electron.*, vol. 56, no. 2, pp. 439-451, Feb. 2009.

[23] J. Hu and Y. He, "Reinforced Control and Operation of DFIG-Based Wind-Power-Generation System Under Unbalanced Grid Voltage Conditions," *IEEE Trans. Energy Convers.*, vol. 24, no. 4, pp. 905-915, Dec. 2009.

[24] S. Buso and P. Mattavelli, Digital Control in Power Electronics. San Rafael, CA, USA: Morgan & Claypool, 2006.

[25] C. Liu, F. Blaabjerg, W. Chen, and D. Xu, "Stator current harmonic control with resonant controller for doubly fed induction generator," *IEEE Trans. Power Electron.*, vol. 27, no. 7, pp. 3207–3220, Jul. 2012.

[26] Y. Song and H. Nian, "Enhanced grid-connected operation of DFIG using improved repetitive control under generalized harmonic power grid," *IEEE Trans. Energy Convers*., vol. 30, no. 3, pp. 1019–1029, Sep. 2015.

Bo Pang was born in Guoyang, China, in 1994. He received the B.Eng. degree from the College of Electrical Engineering, Zhejiang University, Hangzhou, China, in 2016, where he is currently working toward the PhD degree.

His research interests include wind power generation system and doubly fed induction generator control under non-ideal grid.

Heng Nian (M'09 , SM'14) received the B.Eng. degree and the M.Eng. degree from HeFei University of Technology, China, and the Ph.D. degree from Zhejiang University, China, in 1999, 2002, and 2005 respectively, all in electrical engineering. From 2005 to 2007, he was as a Post-Doctoral with the College of Electrical Engineering, Zhejiang University, China.

Since 2016, he has been a Full Professor at the College of Electrical Engineering, Zhejiang University, China. From 2013 to 2014, he was a visiting scholar at the Department of Electrical, Computer, and System Engineering, Rensselaer Polytechnic Institute, Troy, NY. His current research

interests include the optimal design and operation control for wind power generation system. He has published more than 60 IEEE/IET Transaction papers and holds more than 20 issued/pending patents.

Chao Wu was born in Hubei Province, China. He received the B.Eng. degree from HeFei University of Technology, Hefei, China and the Ph.D. degree from Zhejiang University, Hangzhou, China, in 2014 and 2019, both in electrical engineering. He is currently a Postdoctoral Researcher in the Department of Energy Technology, Aalborg University, Aalborg, Denmark.

His current research interests include motor control with power electronics devices in renewable-energy conversion, particularly the control and operation of doubly fed induction generators for DC connection.

Frede Blaabjerg (S'86–M'88–SM'97–F'03) was with ABB-Scandia, Randers, Denmark, from 1987 to 1988. From 1988 to 1992, he got the PhD degree in Electrical Engineering at Aalborg University in 1995. He became an Assistant Professor in 1992, an Associate Professor in 1996, and a Full Professor of power electronics and drives in 1998. From 2017 he became a Villum Investigator. He is honoris causa at University Politehnica Timisoara (UPT), Romania and Tallinn Technical University (TTU) in Estonia.

His current research interests include power electronics and its applications such as in wind turbines, PV systems, reliability, harmonics and adjustable speed drives. He has published more than 600 journal papers in the fields of power electronics and its applications. He is the co-author of four monographs and editor of ten books in power electronics and its applications.